Viewing the Born Model for Ion Hydration through a Microscope

FUMIO HIRATA, PAUL REDFERN, and RONALD M. LEVY
Department of Chemistry, Rutgers University, New Brunswick, New Jersey 08903, USA

Abstract

The hydration-free energy, energy, and entropy of monovalent ions are calculated using the extended RISM integral equation theory and computer simulations. Plots of these thermodynamic quantities against $1/R$, where R is the Lennard–Jones radius, lie on two distinct curves corresponding to cations and anions. This result is attributed to differences in the microscopic structure of solvent surrounding the ions. Charge distribution functions are used to analyze solvent structure. It is found that the modified Born formula proposed by the Latimer et al. gives good agreement with the RISM results for the energy and the free energy, but not for the entropy. A microscopic interpretation of Latimer formula is attempted in light of the statistical mechanical theory.

Introduction

Achieving a quantitative understanding of the behavior of electrically charged species in condensed phases has occupied a central place in physical chemistry for over a century. In the present era, modern statistical mechanical theories of electrolyte solutions have stressed a conceptual framework built upon a detailed picture of the molecular structure of solute and solvent molecules and potentials which describe the interactions between these species. Yet despite the emphasis in some circles on detailed atomic models, continuum electrostatic theories are still widely employed to interpret experiments; with respect to the biophysical chemistry of macromolecular solutions, continuum electrostatic models are enjoying a resurgence of enthusiasm [1–3]. Since there can be no question that theories based on detailed atomic models start from a more fundamental viewpoint, the strength of continuum models lies in the relative ease with which formulas may be derived and applied. However, caution should be exercised when attempting to develop a microscopic interpretation of the parameters contained in the macroscopic theory.

One of the first and simplest problems to be treated by continuum theory concerns the solution thermodynamics of hydrated ions. Born used classical electrostatics to evaluate the free energy change upon transfer of ions from the vacuum to solution [4]. In this very simple model the ions are represented as charged hard spheres and the solvent as a structureless fluid with uniform macroscopic dielectric, which is unperturbed even in the presence of ionic fields. This model leads to the following (Born) equation for the solvation free energy:

$$\Delta F_{\text{Born}} = \frac{Z^2}{2a}\left(\frac{1}{D} - 1\right) \tag{1}$$

International Journal of Quantum Chemistry: Quantum Biology Symposium, 15, 179–190 (1988)

CCC 0360-8832/88/010179-12$04.00

where Z is the charge on the ion, D is the dielectric constant of the solvent, and a is interpreted as an ionic radius. When Pauling's crystal radii (R_X) and macroscopic dielectric constant are employed for a and D, the equation gives values for ΔF which are too large, especially for cations. Since the equation includes only two parameters a and D for characterizing the system, other than the charges which are fixed for ions of the same valence, attempts at improving the theory have been made along two lines, either finding a better set of ion radii or taking account of dielectric saturation effects of solvent near the ions. It was found empirically by Latimer et al. that adding 0.85 Å to the crystal radii of cations and 0.1 Å to those of anions leads to good agreement with experimental [5]. Quite recently, Rashin and Honig reexamined the Born model [6]. They argued that instead of using the ionic radius in the Born equation it was more appropriate to use a "cavity radius" which is defined as "a sphere which contains a negligible electron density contribution from the surrounding solvent." They concluded that the covalent radii provide a good measure of the cavity radii of cations while the crystal radii are appropriate for anions. The cavity radii so defined turn out to be very close to the parameters employed by Latimer et al. Use of cavity radii correlates the hydration enthalpies of more than thirty individual ions with different charge types along a single line. However, attempts to develop a microscopic picture for this essentially macroscopic model raise several questions. Is an extremely detailed microscopic analysis of the Born a parameter justified when the solvent is viewed as structureless? Does the Born model successfully account for the solvation of ions in solvents which have similar dielectric constant but very different microscopic structure? Are thermodynamic quantities really symmetric for cations and anions as implied in the Born equation? The last question is especially important considering the fact that a classical way of partitioning thermodynamic quantities for a salt into individual ions are based upon a similar hypothesis: ions with equal radii should give the same contribution to thermodynamic quantities regardless of their sign [7]. Some of these questions cannot be answered by macroscopic theory but require the methods of statistical mechanics for clarification.

Here we report the results of calculations of the hydration free energy of ions using the extended RISM integral equation and computer simulations, two of the most powerful statistical mechanics methods for studying hydrogen-bonded liquids and their solutions [8–10].

Method

Simulation

Molecular dynamics simulations were performed on systems containing an ion and 215 water molecules in a cubic box with dimensions 18.62 Å per edge. A time step of 0.002 ps was used. After equilibration for 40 ps, trajectories were collected for analysis. The temperature was kept constant by coupling to a heat bath [11]. An 8.0 Å cutoff was used with periodic boundary conditions. Simulations were carried out for Na^+ in water and Cl^- in water. The effect of varying the cation and anion radii on solvation free energy differences was obtained by applying the thermodynamic

pertubation simulation formulas to the Na^+ and Cl^- simulations [12]

$$\Delta\Delta F = \Delta F_f - \Delta F_i = -k_B T \ln\langle\exp\{-(V_f - V_i)/k_B T\}\rangle_i , \tag{2}$$

where ΔF_f and ΔF_i are the free energy of the final and initial states, V_f and V_i are the corresponding potential energies, k_B the Boltzmann constant and $\langle \ldots \rangle_i$ means statistical average over the initial state. For each ion, the results of 10 trajectories each lasting 1000 steps were averaged to obtain mean values for free energy differences, the standard deviation of the mean was used to estimate the statistical uncertainty in the computed free energy differences.

RISM Calculation

The excess free energy change associated with coupling (or charging) an ion in solvent is calculated by the Singer–Chandler equation [13] or its modified version [14]

$$\Delta F_i/k_B T = \sum_s \rho_s \int_0^\infty 4\pi r^2 \left\{ \frac{1}{2} h_{is}^2(r) - c_{is}(r) - \frac{1}{2} h_{is}(r) c_{is}(r) \right\} dr \tag{3}$$

where the subscripts i and s specify ions and solvent sites, respectively. The $h_{is}(r)$ is the site–site total correlation function defined from the site–site pair correlation function $g_{is}(r)$ by

$$h_{is}(r) = g_{is}(r) - 1 , \tag{4}$$

and the $c_{is}(r)$ is defined by the RISM equation

$$h_{is}(r) = c_{is}(r) + \sum_{s'} \rho_{s'} \int c_{is'}(|\mathbf{r} - \mathbf{r}'|) h_{s's}(\mathbf{r}')\, \mathbf{dr}' \tag{5}$$

where $h_{ss'}$ is the site–site total correlation function for the solvent. The renormalized version of eq. (5) supplemented by the HNC closure is solved for h_{is} and c_{is} with a standard iterative procedure explained elsewhere [15]. The entropy is calculated from the free energies at two temperatures using a finite difference equation [15, 16]

$$\Delta S_{298} = -\frac{\Delta F_{300} - \Delta F_{296}}{4} \tag{6}$$

The energy is obtained from eqs. (3) and (6) by

$$\Delta E = \Delta F + T\Delta S \tag{7}$$

The 12–6–1 type potential is used throughout the calculation [10]. The SPC model with slight modification is used for solvent molecules [11, 18, 19], while the Lennard–Jones parameters given by Jorgensen and co-workers [20] are employed for Na^+ and Cl^-. The parameters are listed in Table I. A series of calculations are performed changing the ionic radii which is defined to be $(\sigma/2)$, where σ is the Lennard–Jones diameter.

Results and Discussion

We first examine the shape of the interaction potential between an ion and a single water molecule in the present model. The plots of the interaction energy between

TABLE I. Nonbonded parameters.

Species	σ (Å)	ε (kcal/mol)	Z (electronic charges)
Na^+	1.897	1.607	1.0
Li^+	1.26	6.25	1.0
Cl^-	4.410	0.118	−1.0
O	3.166	0.1554	−0.82
H	1.0	0.055	0.41

[a](12–6–1) potential: $U_{ij}(r) = 4\varepsilon_{ij}[(\sigma_{ij}/r)^{12} - (\sigma_{ij}/r)^6] + Z_iZ_j/r$, $\sigma_{ij} = (\sigma_{ii} + \sigma_{jj})/2$, $\varepsilon_{ij} = \sqrt{\varepsilon_i\varepsilon_j}$

[b]SPC water model: r(OH) = 1.0 Å, ∠HOH = 109.47°.

$Li^+Na^+Cl^-$ and water are shown in Figure 1 as a function of ion–oxygen separations. Also, shown are plots of the interaction energies for hypothetical ions with the same Lennard–Jones parameters but opposite charge (e.g., "Li^-," "Na^-," "Cl^+"). In all the figures the angle between the ion–oxygen vector and the water dipole vector has been

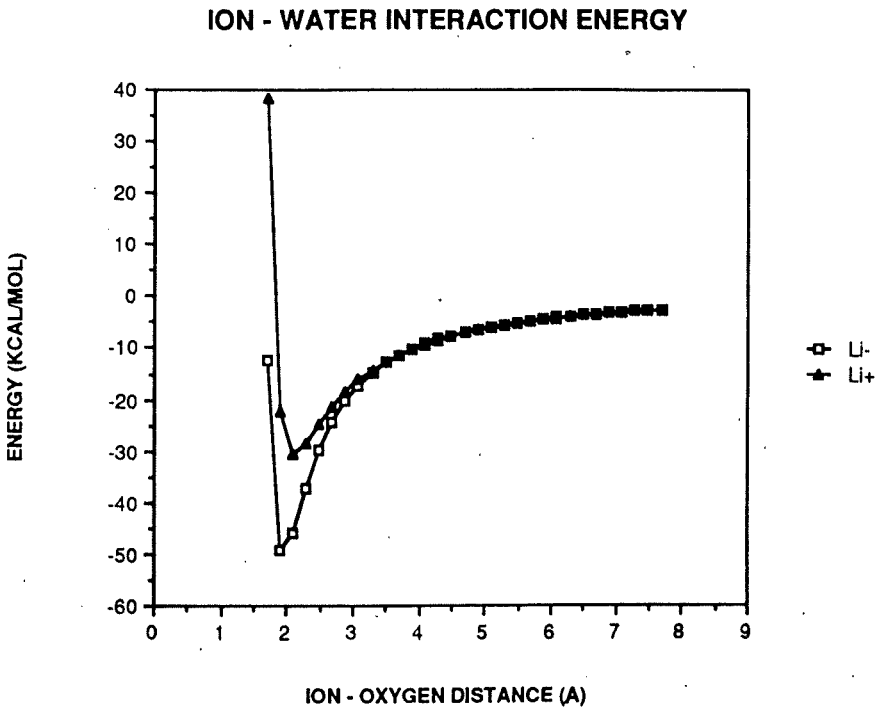

(a)

Figure 1. Ion–water monomer interaction potential as a function of ion oxygen separation. The angle between the ion–oxygen dipole vector and the water dipole vector has been optimized. The Lennard–Jones parameters correspond to (a) Li (b) Na, (c) Cl. The anionic form (open symbols), and the cationic form (closed symbols).

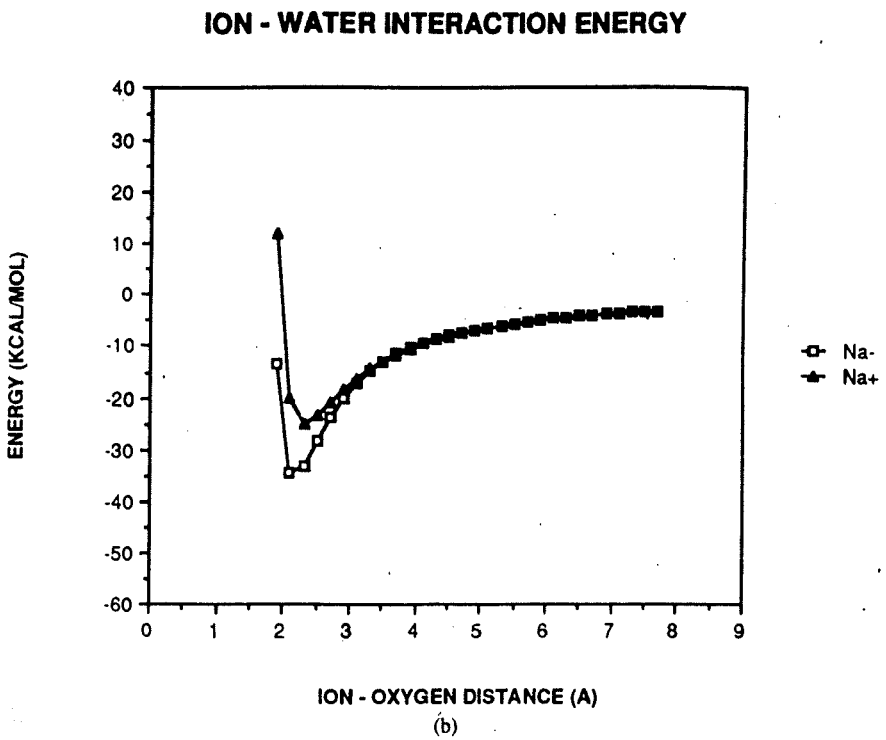

(b)

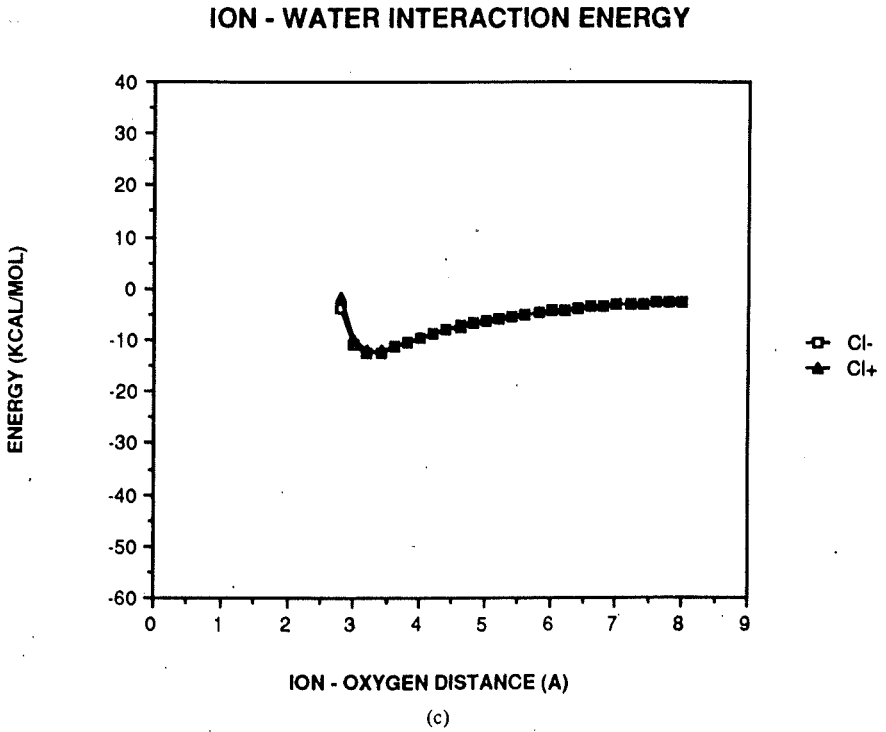

(c)

Figure 1. continued

optimized. For positive ions, by symmetry, the ion–oxygen vector lies on the axis which bisects the HOH angle, with the water protons pointed away from the positive ion. For the negative ions however, the minimum energy geometry does not correspond to one in which the ion is equidistant from the two water protons. For the smaller anions ("Li^-," "Na^-"), the minimum energy ion–water geometry corresponds to an almost linear hydrogen bond (the water—OH bond lies 5° off the ion–oxygen axis); while for the chloride–water interaction, the water—OH bond lies 20° off the ion–oxygen axis in the minimum energy geometry. The angular dependence of the ion–water molecule interaction energy at the minimum energy internuclear separation is shown in Figure 2. It is clear from the figures that for a given set of Lennard–Jones parameters, at the minimum energy geometry, the anion–water monomer interaction is more attractive than the corresponding cation–water energy. For example, the "Na^-"–H_2O energy is 12 kcal/mol more attractive at the minimum than the Na^+–H_2O interaction energy. As the ion radius increases, the difference between anions and cations decreases. For an ion with Lennard–Jones radius corresponding to Cl, the ion–water interaction energy of the anionic species (Cl^-) and the cationic species ("Cl^+") are the same [Fig. 1(c)] at the optimum geometry. Thus, for larger ion–water separations, the Coulomb interaction between an ion and a single water molecule is adequately represented by a monomer–dipole interaction. From the analysis of the model potential surface for the interaction of an ion with a single water monomer, it is seen that for small ions, the anion is differentially stabilized compared with the corresponding cation. As the ion radius increases, this differential effect is diminished. While condensed phase effects cannot be interpreted on the basis of the structure of the ion–water monomer potential surface because of the complex many body effects which determine the structure of the solutions, it should be noted that the ion–water monomer potentials are very deep and this suggests that some features of the ion–water monomer potential may be reflected in the condensed phase results.

We turn now to an examination of the ion hydration thermodynamics using both RISM integral equation and computer simulation methods. The ΔF, ΔE, and $T\Delta S$ calculated using eqs. (3), (6), and (7) are plotted against the inverse of the ionic radii in Figure 3. A striking feature of the plot is that ΔF for cations and anions lie on different curves in contrast to the Born equation. For a cation and an anion of the same radius, the charging free energy change is much larger in magnitude for the anion than for the cation. As the ion radius increases, the difference in the solvation free energy between an anion and a cation of equal radius decreases. The corresponding effect was observed for the ion–water monomer interaction potential discussed above; however quantitative aspects of the solution thermodynamics cannot be estimated from the ion–water potential. For example, in solution the difference in the solvation free energy between Na^+ and "Na^-" is 50 kcal/mol, that is more than three times the values for the isolated ion–water pair. It should be emphasized that the difference in the thermodynamics between anions and cations has nothing to do with the choice of ionic radii but emerges from the asymmetric nature of the ion–solvent interaction. To see this more closely, charge distribution functions (CDF) defined as

$$Q_i(r) = \sum_s Z_s \rho_s g_{is}(r) 4\pi r^2 \tag{8}$$

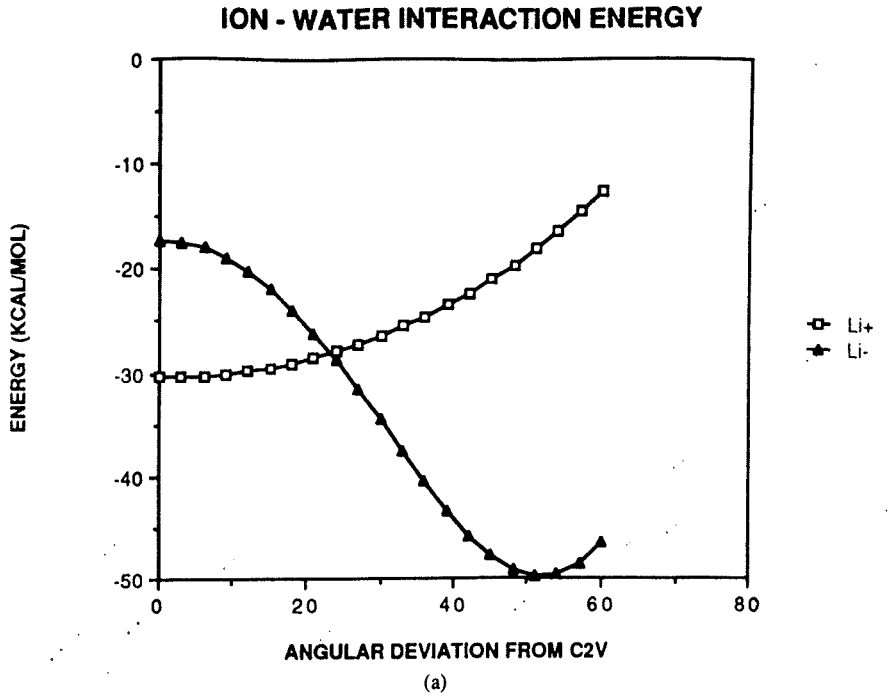

(a)

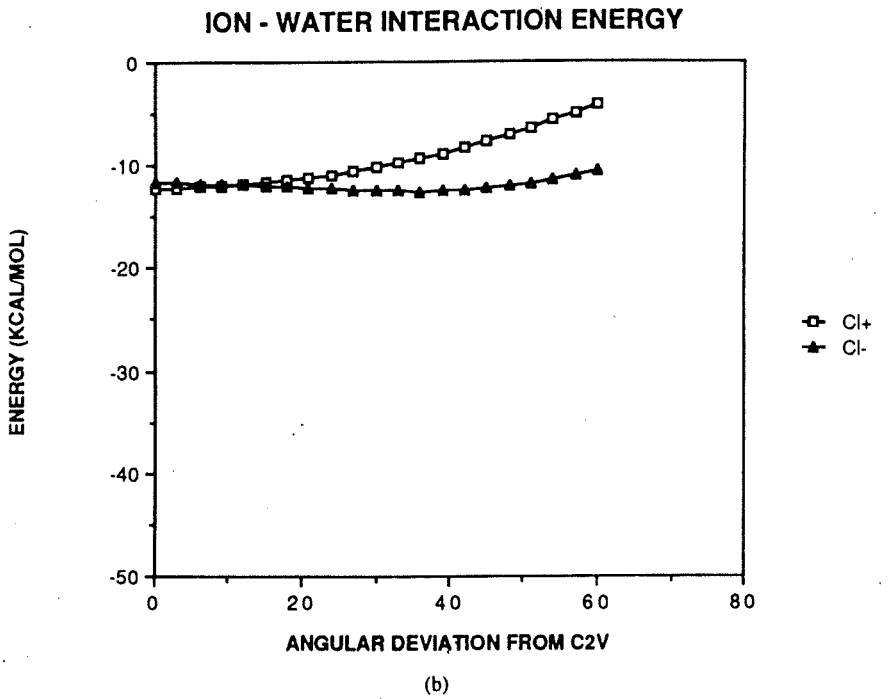

(b)

Figure 2. Ion–water monomer interaction energy as a function of the angle between the ion–oxygen vector and the ion–dipole vector. The ion–oxygen internuclear distance has been optimized. The Lennard–Jones parameters correspond to (a) Li, (b) Cl. The anionic form (open symbols), the cationic form (closed symbols).

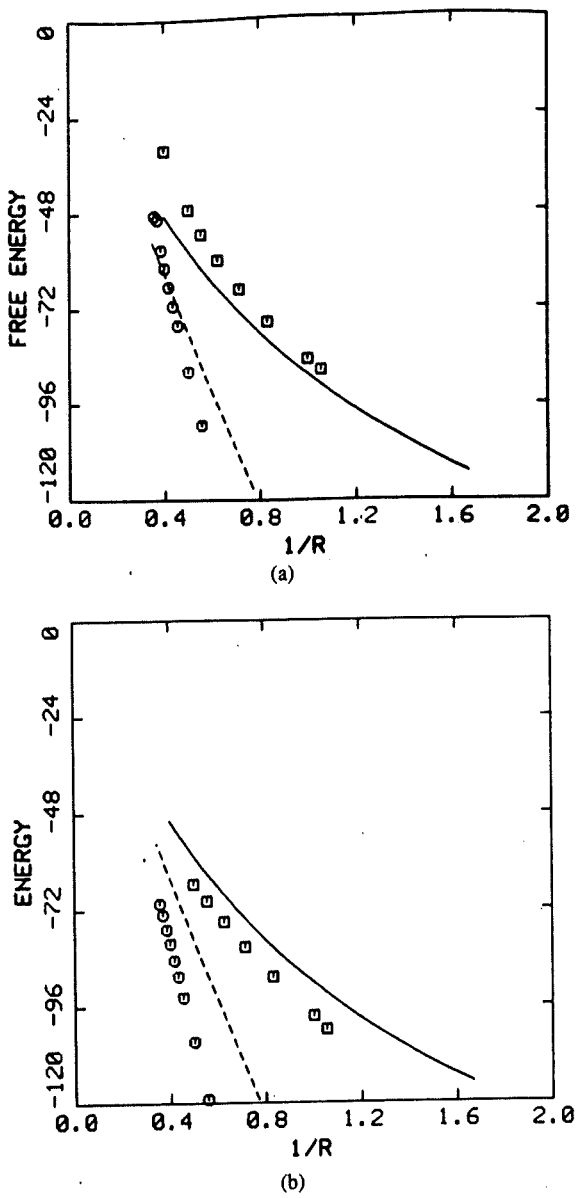

Figure 3. (a) ΔF, (b) ΔE, and (c) $T\Delta S$ calculated from the RISM and the Latimer–Pitzer–Slansky (LPS) equations: (—) cations (LPS), (- - -) anions (LPS); (□) cations (RISM); (○) anions (RISM).

are plotted in Figure 4. In the equation, Z_s stands for the partial charges on the sites (O, H) of water molecules. As may be seen, the population of charges with opposite sign becomes largest in the vicinity of ions and the CDF exhibits a marked oscillation as the ion center–solvent site distance changes. The most interesting difference in the

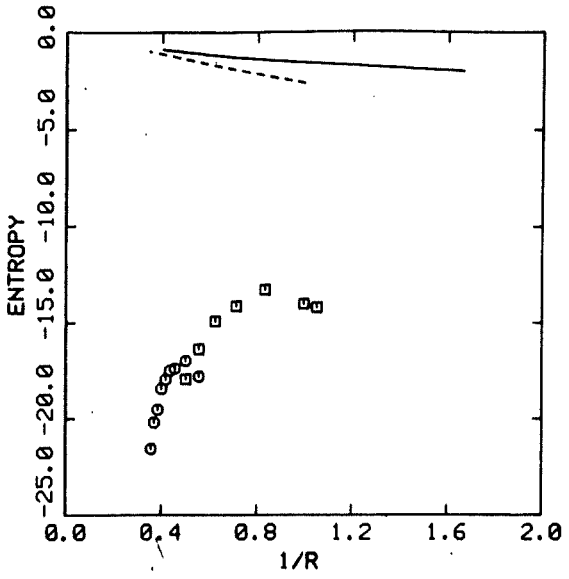

(c)

Figure 3. continued

curves between cations and anions is in the location of the first peak (positive or negative). For ions with the same radius, the first peak position is much shorter for anions than for cations. For example, for the ions with a Lennard–Jones radius of 2.0 Å, it is ca. 2.1 and 3.5 Å for anions and cations, respectively. The asymmetric feature in the CDF is a consequence of the very different hydration structure corresponding to the two types of ions, i.e., cations are primarily solvated by nearest neighbor water oxygen atoms while for the anions water protons are the nearest neighbors. Since the oxygen has a large core while hydrogens have virtually no cores and are arranged at the surface of the oxygen sphere, the anion nearest neighbor oxygen distance is larger than the corresponding cation nearest neighbor water proton distance for two ions with the same radius. Considering that the dominant contribution to the electrostatic energy comes from the first peak, it is clear that the difference in the solvation free energy between anions and cations is a consequence of the difference in the hydration structure of the two types of ions. In this connection, it is of interest to plot the results from the Latimer–Pitzer–Slansky (LPS) equation [5]. For the free energy it is

$$\Delta F_{\mathrm{LPS}} = \frac{Z^2}{2(a + \Delta)}\left(\frac{1}{D} - 1\right) \tag{9}$$

where Δ is an empirical parameter. Results are shown in Figs. 3(a)–(c) with $a = R$ and Δ is 0.85 and 0.1 Å for cations and anions, respectively. As may be seen, the LPS equation agrees very well with the RISM prediction for ΔE and ΔF implying that the empirical parameter is interpreted as a correction to the continuum model due to the microscopic structure of solvents. The same interpretation for Δ has been

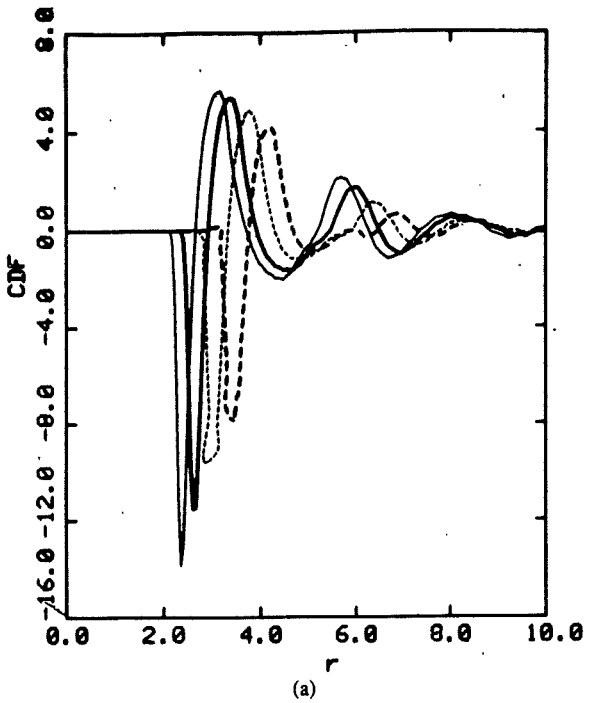

(a)

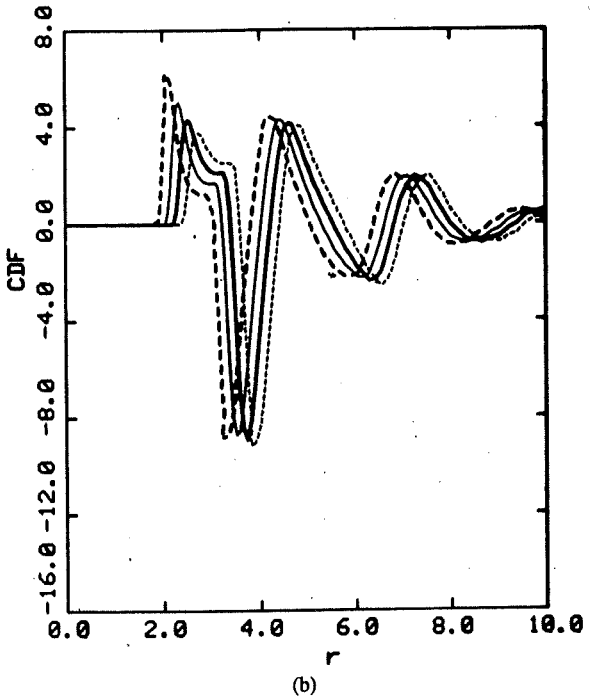

(b)

Figure 4. (a) Charge distribution functions (CDF) around cations: thin solid line, R = 0.9485 Å; thick solid line, R = 1.2 Å; thin dashed line, R = 1.6 Å; thick dashed line, R = 2.0 Å. (b) Charge distribution function (CDF) around anions: thick dashed line, R = 2.0 Å; thin solid line, R = 2.205 Å; thick solid line, R = 2.4 Å; thin dashed line, R = 2.6 Å.

found by Chan et al. based upon the analytical solution of the MSM (mean spherical model) equation for the ion–dipolar system in which the solvent molecules are hard spheres with point dipoles at the center [21]. In light of those results, the cavity radii introduced by Rashin and Honig, which is apparently equivalent to $(a + \Delta)$ in eq. (9), should be regarded as a size parameter which *effectively* takes into account the microscopic solvent structure.

A marked difference between RISM and LPS predictions is observed for $T\Delta S$ (Fig. 3(c)). Since both the experimental value and the semiempirical theory have not been well established for these quantities, it is not possible at present to evaluate the results quantitatively. Nevertheless, there are two interesting qualitative differences between the two theories, RISM and LPS, which we point out. Firstly, The RISM theory produces much a greater dependence of the hydration entropy on both the charge type and the ion size than the continuum theory does. This may be because in the LPS theory the temperature dependence in the free energy comes solely from the dielectric constant or the long range contribution, while the short range contribution is taken into account as well in the RISM theory. Secondly, the LPS theory predicts linear dependence of the entropy on $(1/R)$, whereas the RISM theory shows much more complicated behvior. For both cations and anions, there is a maximum in the entropy as functions of the inverse of the ionic radius; the entropy decreases as the ionic radius increases or decreases. The small R behavior, wherein the solvent becomes more ordered around the small ion, is apparently a manifestation of the standard electrostatic effect [22]. The large R behavior is apparently a form of "hydrophobic hydration" which has been observed not only for neutral species but large charged species as well such as alkylammonium ions [23].

Questions arise about the RISM thoery results because the thoery is known to give the incorrect dielectric constant [24]. Nevertheless, the results agree well with experiment as fit by the semiempirical LPS equation [Eq. (9) and Fig. 3]. We note also the RISM theory agrees well with the results of our comupter simulations (Table II). This agreement undoubtedly reflects the relative importance of the short range versus the long range solvent contributions to the ion solvation free energy. It is known that RISM theory predicts the short range ion solvent structure well [16, 19]. In this regard we note that the formal solution for free energy of the dipole hard-sphere model may be factored into an expression with the form of Eq. (9) [21]. The two parameters D and Δ embody solvent characteristics. The dielectric constant represents the long range contribution to the free energy, while Δ represents a short range contribution. Note that the factor $(1/D - 1)$ is a very insensitive function of D so that a tenfold variation in D of between 8 and 80 leads to only a 10% variation in $(1/D - 1)$ between 0.875 and 0.988. This difference changes the free energy by only 12%. The free energy is much more sensitive to the short range contribution Δ.

TABLE II. Molecular dynamics computer simulation results for ion solvation free energy differences.

Ion	σ	$\Delta\sigma$	$\Delta\Delta F$	$\Delta\Delta F$ (RISM)
Na^+	1.897	0.2	6.18 ±0.53	+5.18
Cl^-	4.410	−0.41	−11.123 ±0,56	−14.18

While the solution to the dipole hard-sphere model may be expressed in the form of Eq. (8) in which the short and long range solvent contribution to the free energy are clearly identified, it would be of interest to find a corresponding analytical expression for the RISM equation.

Acknolwedgment

This work has been supported by the National Institute of Health (GM-30580), the Petroleum Research Fund of the American Chemical Society, the National Science Foundation Office of Advanced Scientific Computing, and the John Von Neumann Supercomputer Center.

References

[1] J. Warwicker and H. C. Watson, J. Mol. Biol. **157**, 671 (1982).
[2] M. K. Gilson, A. A. Rashin, R. Fine, and B. Honig, J. Mol. Biol. **183**, 503 (1985).
[3] M. K. Gilson and B. Honig, Nature **330**, 84 (1987).
[4] M. Born, Z. Phys. **1**, 45 (1920).
[5] W. M. Latimer, K. S. Pitzer, and C. M. Slansky, J. Chem. Phys. **7**, 108 (1939).
[6] A. A. Rashin and B. Honig, **89**, 5588 (1985).
[7] G. Kortum and J. O'M. Bockris, *Textbook of Electrochemistry* (Elsevier, New York, 1951).
[8] D. Chandler and H. C. Andersen, J. Chem. Phys. **57**, 1930 (1972).
[9] F. Hirata and P. J. Rossky, Chem. Phys. Lett. **84**, 329 (1981).
[10] P. J. Rossky, Ann. Rev. Phys. Chem. **36**, 321 (1985).
[11] H. J. C. Berendsen, J. P. M. Postma, W. F. von Gunsteren, and J. Hermans, *Intermolecular Forces*, B. Pullman, Ed. (Reidel, Dordrecht, 1981).
[12] T. Lybrand, I. Ghosh, and J. A. McCammon, J. Am. Chem. Soc. **107**, 7793 (1985).
[13] S. J. Singer and D. Chandler, Mol. Phys. **55**, 621 (1985).
[14] D. A. Zichi and P. J. Rossky, J. Chem. Phys. **84**, 1712 (1986).
[15] F. Hirata, P. J. Rossky, and B. M. Pettitt, J. Chem. Phys. **78**, 4133 (1983).
[16] B. M. Pettitt and P. J. Rossky, J. Chem. Phys. **84**, 5836 (1986).
[17] C. L. Brooks III, J. Chem. Phys. **86**, 5156 (1987).
[18] W. L. Jorgensen, J. Chandrasekhar, J. D. Madura, R. W. Impey, and M. L. Klein, J. Chem. Phys. **79**, 926 (1983).
[19] F. Hirata and R. M. Levy, J. Phys. Chem. **91**, 4788 (1987).
[20] (a) W. L. Jorgensen, J. Am. Chem. Soc. **103**, 335 (1981).
(b) J. Chandrasekhar, D. C. Sellmeyer, and W. L. Jorgensen, J. Am. Chem. Soc. **106**, 903 (1984).
[21] D. Y. C. Chan, D. J. Mitchell, and B. W. Ninham, J. Chem. Phys. **70**, 2946 (1979).
[22] H. S. Frank and W. Y. Wen, Discuss. Faraday Soc. **24**, 133 (1957).
[23] J. Y. Huot, Jolicoeur, *The Chemical Physics of Solvation (part A. Theory of Solvation)*, R. R. Dogonadze, E. Kalman, A. A. Kornyshev, and J. Ulstrup, Eds. (Elsevier, New York, 1985). p. 417.
[24] D. Sullivan and C. G. Gray, Mol. Phys., **42**, 443 (1981).

Received May 3, 1988